JOURNAL OF MATERIALS SCIENCE 29 (1994) 6231–6240

Diffusional penetration during diffusion-induced grain-boundary migration process in an Al–Zn couple

P. ZIEBA, A. PAWŁOWSKI
Institute of Metallurgy and Materials Science of the Polish Academy of Sciences, 25 Reymonta Street, 30–059 Cracow, Poland

The existence of diffusion-induced grain-boundary migration (DIGM) has been re-examined by electron probe micro analysis and analytical electron microscopy in the aluminium substrate of Al–Zn diffusion couple annealed in the temperature range 395–535 K. The investigation revealed two basic kinds of DIGM: laminar and turbulent. The laminar kind occurs over the whole temperature range and is characterized by a small migration distance and large migration depth. The zinc enrichment at a sample surface is 4.0–5.0 wt% and gradually decreases with increasing depth. The turbulent kind is limited to annealing temperatures above 450 K. In this case, the width of the alloyed zone is much greater, close to the surface of sample and then dramatically decreases, showing a behaviour similar to the laminar morphology. The zinc content at the surface of sample is 8.0–9.0 wt%. The diffusivities of DIGM calculated based on Cahn's equation agree well with the values of stationary grain boundary in diluted AlZn alloys. Evidence for the existence of DIGM was the asymmetry of the zinc profile with regard to the final position of the boundary. Microanalytical scan across the alloyed zone showed an abrupt change of the zinc concentration at the moving boundary. This suggests that the role of volume diffusion during DIGM is not so important and a considerable chemical contribution to the total driving force should exist.

1. Introduction

It is well established that the diffusion of solute atoms along the grain boundary can force the boundary to migrate leaving behind a solute-enriched zone. This phenomenon, known as diffusion-induced grain-boundary migration (DIGM), has been extensively studied in binary systems such as Fe–Zn [1–6], Cu–Zn [7–13] and Cu–Ni [14–18].

The Al–Zn system seems to be an ideal system for the study of the DIGM process because other phenomena at the moving boundaries were observed over a wide range of temperatures and zinc concentrations. Tashiro and Purdy [19, 20] reported that DIGM occurs in this system with an extensive volume diffusion ahead of the migrating boundaries. The rates of migration were very slow, being about two orders of magnitudes lower than during discontinuous precipitation at corresponding temperatures. Therefore, Tashiro and Purdy proposed the driving force of DIGM resulting from the coherency strain in the zinc concentration profile ahead of the boundary. A recent investigation of Varadarajan and Fournelle [21] doubted whether the observed migration was due to DIGM or simply due to the normal migration process.

The present work was undertaken in order to obtain more experimental information. The following features typical for DIGM occurrence were examined:

1. the formation mechanism of the zinc-enriched zone behind the moving boundary;
2. the morphology of the new zinc-enriched zone at various depths and over various distances to which the boundary migrates;
3. the level of zinc enrichment within the new grain, the asymmetry of the zinc profile with respect to the grain boundary, and the step-like change of zinc content at the grain boundary;
4. the value of diffusivity at the moving grain boundary and its comparison with other data on diffusion.

2. Experimental procedure

Aluminium of 99.99% purity was melted in a graphite crucible and cast into a steel mould. The ingot was cut into slabs 5 mm thick and cold rolled to thicknesses of 1.5 and 0.05 mm. Then the samples were annealed at 600 K for 0.5 h. The resulting grain size was about 1500 μm. After annealing the samples were electrodeposited with zinc. Electrodeposition was carried out in an acid bath containing 20 $g l^{-1}$ zinc ions and 10 $g l^{-1}$ HCl. Moreover, 40 $mg l^{-1}$ fluor ions were added in order to improve the adhesion of the zinc

0022–2461

layer to the aluminium substrate. The thickness of the zinc coating was between 8 and 15 μm. Samples 1.5 mm thick were plated on one side (type A), while those 0.05 mm thick were plated on both sides (type B). The geometry of the resultant samples is graphically presented in Fig. 1. The coated diffusion couples were then held at temperatures ranging from 395–535 K.

In order to determine the grain-boundary (GB) migration velocity the apparent width of alloyed zone, w', was taken as a perpendicular distance from original location of the GB to the migrating boundary, using an optical microscope. About 40 to 50 individual measurements were made on the surface of the sample of A type. Prior to measurements, the plated layer of zinc was electrolytically removed using a solution of perchloric acid, ethanol, methylo glycol and glycerol at a potential of 20 V. The values of w' were averaged and multiplied by $\pi/4$ in accord with Lück's [22] method. Finally, the GB migration velocity was obtained from the slopes of w' versus time.

Zinc concentration measurements across DIGM regions were carried out using an electron probe microanalyser (EPMA) with wavelength dispersive spectroscopy. Zinc and aluminium were detected by separate spectrometers and the specimens were oriented in such a way that the take-off angle of X-rays detected was 35°. The zinc and aluminium counts were normalized against a pure zinc and aluminium standard. Within the 95% confidence limit, the measurement error was $\pm$ 4.5%.

The limited spatial resolution of the EPMA method does not allow good resolution of the solute concentration immediately at the front, and just behind the final position of the moving boundary. Therefore, part of the samples were used to prepare thin foils for an electron microscope Philips CM20 Twin equipped with an energy dispersive spectrometer. Energy dispersive X-ray (EDX) analyses were carried out with the microscope operating at 200 kV in the nanoprobe mode and a 50 μm diameter "top hat" condenser aperture. This resulted in a probe size of 10 nm. The average foil thickness calculated based on the contamination spots produced on the top and bottom of the foil, was about 200 nm. During analysis, the specimens were tilted approximately 15° towards the energy dispersive detector which resulted in 35° take-off angle. The intensity of characteristic X-ray peaks, I_{AlK_α} and I_{ZnK_α} were obtained for X-ray acquisitions time of 60 s using a Link eXl energy dispersive spectrometer and the ancillary electronics. Within 95% confidence limit, the measurement error was $\pm$ 12% for the minor element. The weight per cent of zinc at the points analysed was obtained from the observed peak integrals using the Cliff–Lorimer "ratio technique" [23]. In the present study, $K_{Al-Zn} = 1.25 \pm 0.1$ using a homogenized Al21.55 at % Zn standard under similar conditions to those used to obtain the spectra from the annealed samples.

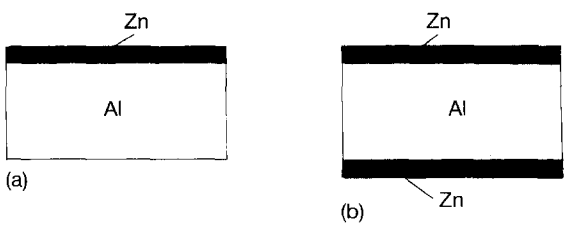

Figure 1 Schematic illustration of diffusion couples used for the experiment: (a) A type sample, (b) B type sample.

3. Results

3.1. Morphology and chemical analysis

Investigation of cross-sectioned samples of A type using an optical microscope and SEM revealed that only a small number of the boundaries had migrated during annealing in the temperature range 395–535 K. At the lowest and the highest temperatures, the migration distances were extremely short and they did not exceed a few micrometres. Therefore, further investigation was focused on samples annealed in the temperature range 415–515 K.

The morphologies of the migrating boundaries were observed to be limited to two basic types. In most cases the grain boundaries moved in a single direction, though bulging into two directions was also noted. The migration distances were usually very small, approximately constant, with the extreme depth to which migration occurred. This is shown by the example of a specimen annealed at 415 K for 10 days (Fig. 2). The migration distances of grain boundaries GB-1, GB-2, GB-3 measured along line A–A are 10, 5 and 8.5 μm, respectively. As the shape of migrating boundaries is not corrugated and the migrating distance decreases gradually with increasing depth below the surface of the specimen, this kind of a process was termed laminar.

The concentration profiles measured across line A–A of Fig. 2 were asymmetric (Fig. 3) with a maximum zinc content at the final position of the boundary. A step-like variation of zinc concentration across the boundary was observed. It should be noted, however, that such a profile shape was partially due to the poor resolution limit of the EPMA. Fig. 4 presents the variation of zinc content with depth for the initial and

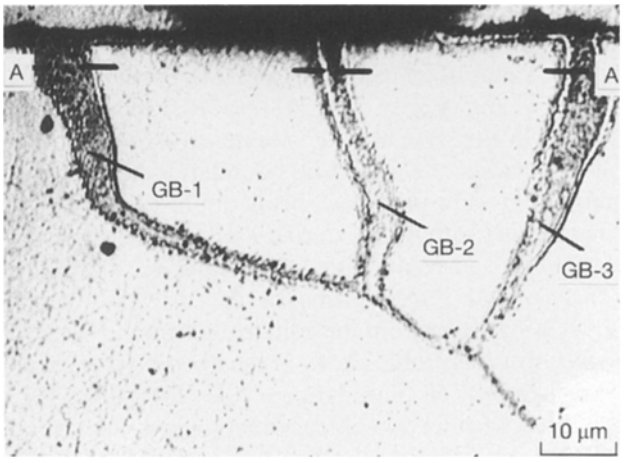

Figure 2 Cross-section of an A type sample annealed at 415 K for 10 days showing migration of the original grain boundaries GB-1, GB-2, GB-3.

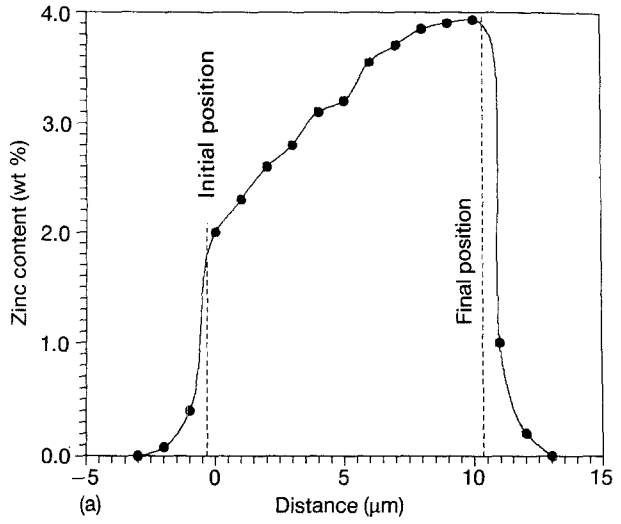

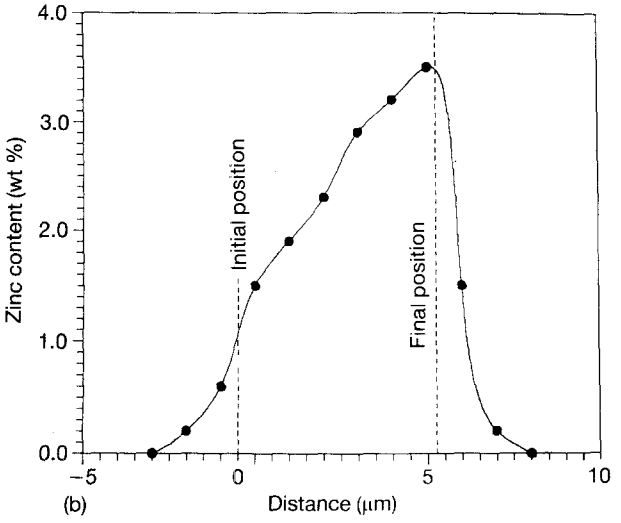

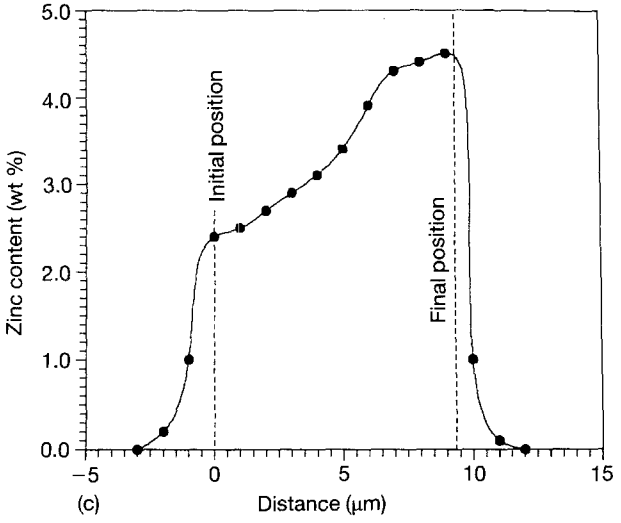

Figure 3(a–c) Zinc concentration profiles along line A–A in Fig. 2.

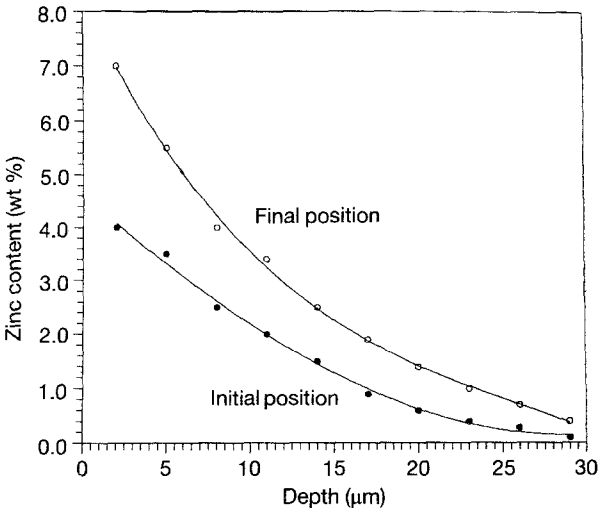

Figure 4 Variation of zinc content with depth for initial and final positions of the boundary denoted GB-1 in Fig. 2.

final positions of the boundary denoted GB-1 in Fig. 2. The concentration decreased monotonically with depth at these two positions of the grain boundary. The concentration at the final position was greater than at the initial one.

At higher temperatures (starting from 455 K) some boundaries were observed to migrate with the distance of migration being much greater, near the diffusion couple interface, than at the sample interior. Such grain-boundary migration was termed turbulent. Fig. 5 presents a micrograph taken after 10 days annealing at 455 K of an A type sample. The migration distances were found to be 55 μm at the interface, decreasing to 25 μm at a depth of 15 μm, and attaining 7 μm at a distance of 75 μm below the Zn/Al interface. It should be noted that the region enriched with zinc did not represent some sort of surface precipitation, because even heavy etching procedure did not remove them from the surface of the specimen. The results of EPMA analysis for the boundary shown in Fig. 5 are presented in Fig. 6a–f. The measurements of zinc concentration along lines A–A, B–B, C–C, D–D, E–E and F–F give profiles across the alloyed zone at depths of 5, 15, 30, 40, 60 and 75 μm below the electrodeposited zinc layer, respectively. The profile taken along the dotted line X–X gives the variation of the zinc content within the alloyed zone as a function of the depth below the sample surface (Fig. 7). An asymmetric shape of the zinc profiles is visible for all the sections presented in Fig. 6. The maximum zinc content corresponds to the final positions of the boundary and it decreases with increasing distance from the coated surface of specimen. This is in agreement with the zinc profile presented in Fig. 7 where appropriate cross-sections are marked by dashed lines.

Therefore, the investigation of cross-sectioned bulk specimens allow two basic kinds of process to be distinguished. The first one, observed over the whole temperature range, is characterized by the small migration distances with extreme depth to which migration occurs. The changes of migration distances along the depth are rather smooth. Zinc enrichment close to the surface of specimens is $\sim$ 4.0–5.0 wt%, with a maximum at the final positions of the boundaries. The solute content gradually decreases with increasing depth both at the initial and final position of the boundary.

The second kind, termed turbulent, is attributed to the higher annealing temperatures (above 450 K). In

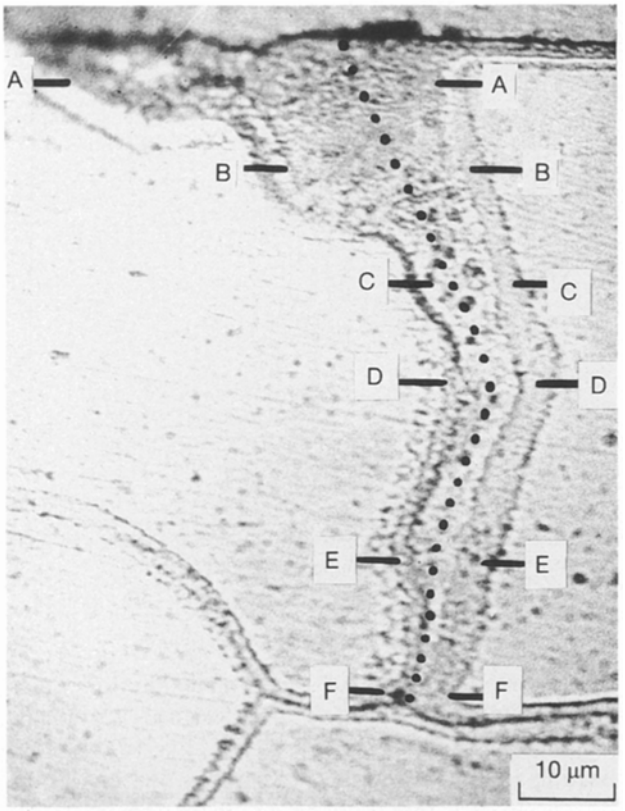

Figure 5 Scanning electron micrograph of an Al–Zn bulk couple annealed at 455 K for 10 days.

this case, the migration distance close to the surface is much larger than at the sample interior. The shape of the migrating boundary is not smooth. Close to the sample surface, the zinc content is twice as high in comparison with the previous morphology. Then, it is observed to decrease with increasing depth, attaining 3.0–5.0 wt% Zn for migration distances typical for laminar morphology.

The region swept by the boundary in Fig. 5 shows grooves which are a result of etching rather than a jerky motion of the boundaries. On the other hand, for some oblique samples (Fig. 8a), the areas left behind the moving boundary were definitely filled with ghost lines. It is expected that after initial movement from position 1 to 2, the boundary started to oscillate, marking successive locations by ghost lines. The final position, denoted by 3, corresponds to the maximum of zinc content (Fig. 8b). Another maximum corresponds to the maximum migration distance (position 2).

Fig. 9a is a TEM image of the alloyed zone close to the edge of the foil annealed at 455 K for 10 days. Fig. 9b is a concentration profile taken along line A–A using energy dispersive X-ray analysis. The beam step increment close to the boundaries of the zinc enriched zone was 0.05 μm. Sharp discontinuities are observed both at the initial and final positions of the boundary. The maximum zinc content is at the final position, which agrees well with the EPMA results. It was very difficult to find a region which would be suitable for EDX analysis. Most of the zinc-enriched regions were in the shape of a wedge which was found by tilting experiments. In such cases, the zinc content would be influenced by the aluminium matrix beneath the alloyed zone and these regions were not subjected to EDX analysis. Therefore, the presented result is one of a few exceptions where EDX analysis could be made correctly. Some zinc content detected outside the alloyed zone may have been due to the presence of zinc atoms which diffused into the surface layers of the aluminium

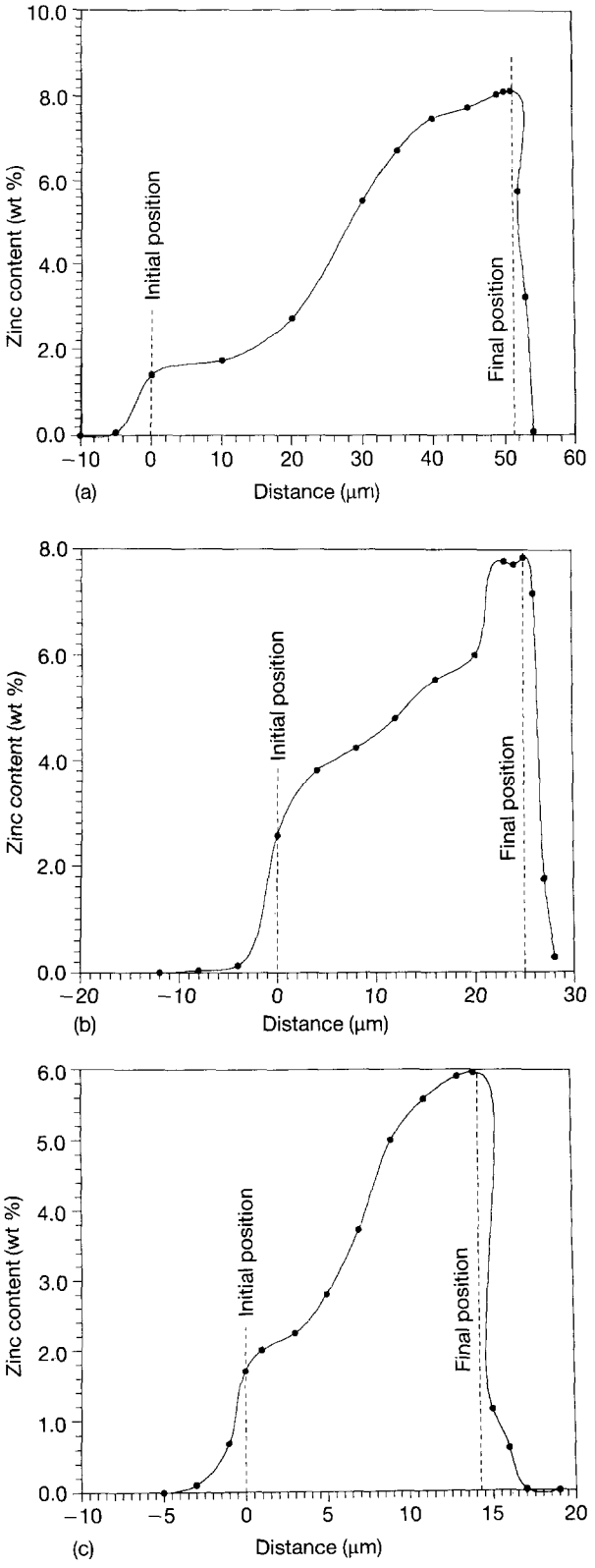

Figure 6 Variation of zinc concentration along lines (a) A–A, (b) B–B, (c) C–C, (d) D–D, (e), E–E, (f) F–F, within the alloyed zone showed in Fig. 5.

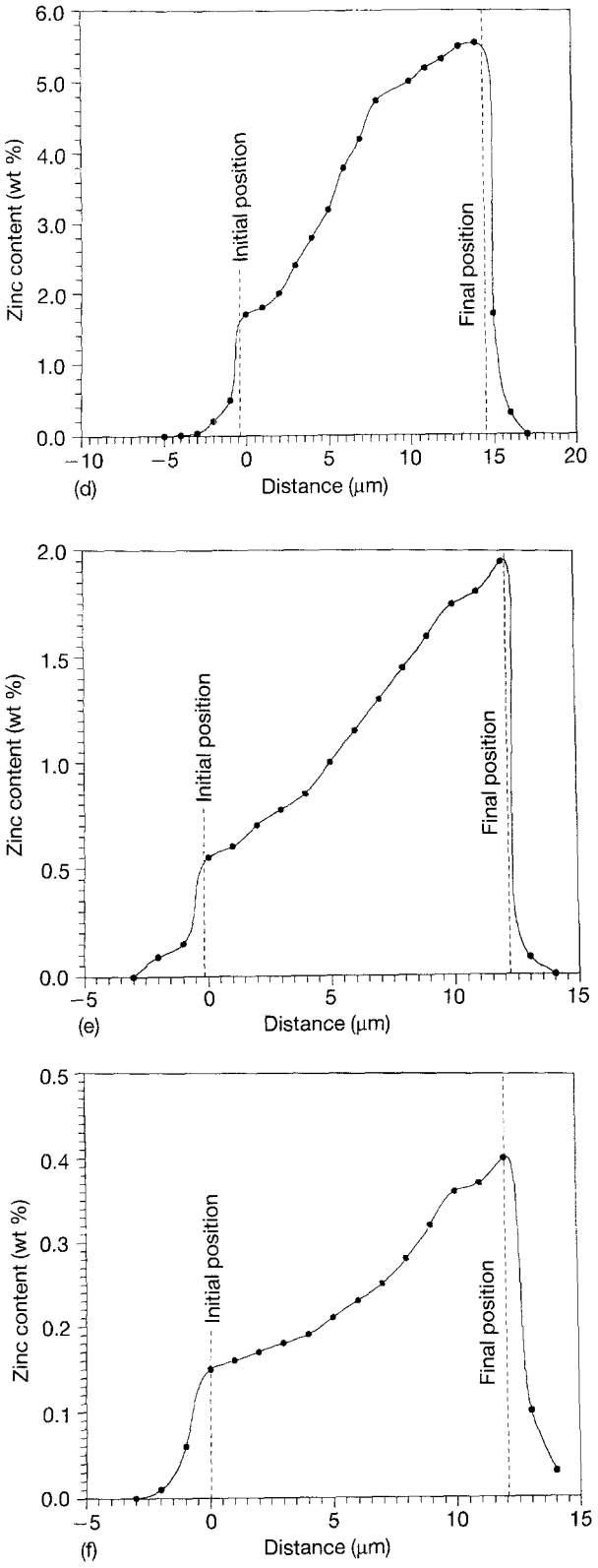

Figure 6 Continued

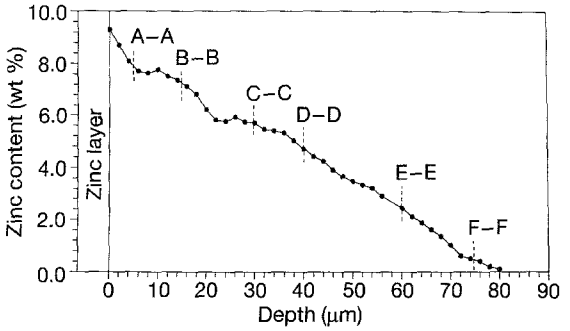

Figure 7 Variation of zinc concentration as a function of the depth below the sample surface (line X–X in Fig. 5).

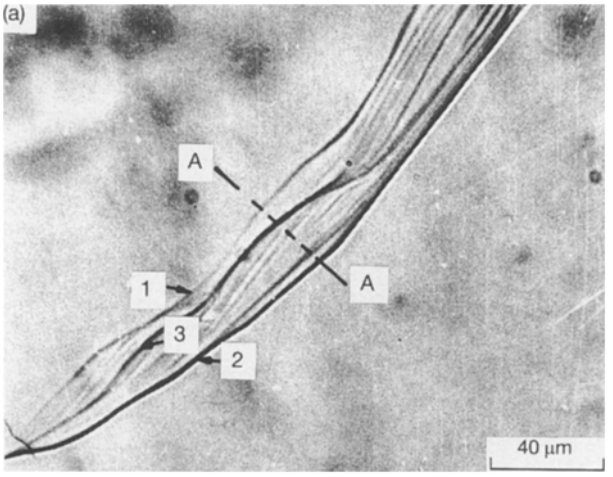

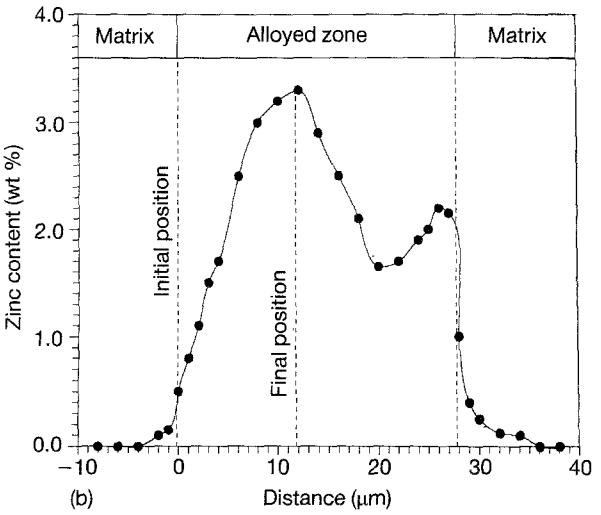

Figure 8 (a) Light micrograph showing DIGM process in an aluminium sample zincified at 475 K for 24 h. 1, The initial position of the boundary; 2, the maximum migration distance; 3, the final position of the boundary. (b) EPMA analysis across line A–A in Fig. 8a.

substrate during annealing of a B type sample. Another possibility may be connected with errors during collecting the zinc spectrum close to the detectability limit of the EDX method.

3.2. Migration rate

Fig. 10 shows the variation of the velocity of GB migration measured at the surface of oblique sections of A type samples annealed in the temperature range 395–535 K. As can be seen, the migration velocity increases with increasing annealing temperature up to maximum at 475 K, then gradually decreases, attaining at 535 K a value comparable to that at the lowest temperature of annealing. GB migration was not observed below 395 K and above 535 K in spite of a considerable number of experiments.

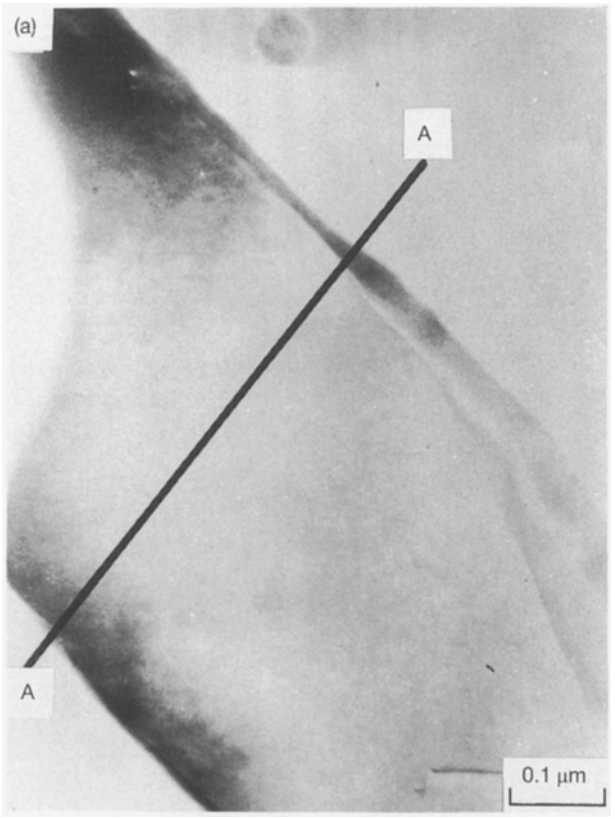

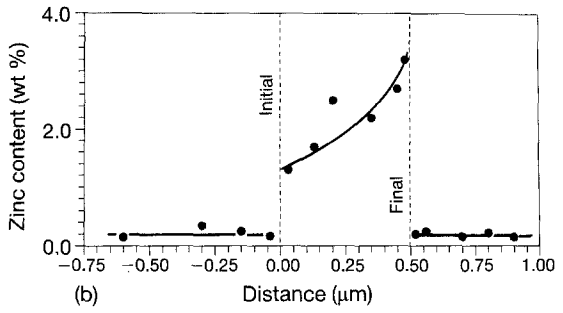

Figure 9 (a) Transmission electron micrograph showing the DIGM process after annealing of a B type sample at 455 K for 10 days. (b) The zinc concentration profile taken along line A–A in (a).

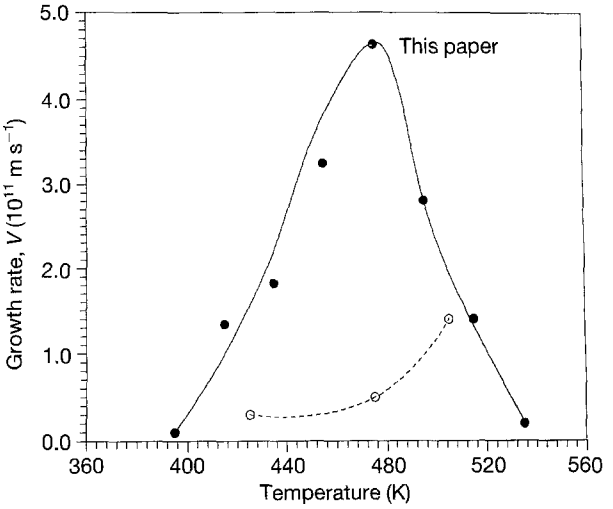

Figure 10 Variation of velocity of grain-boundary migration in the temperature range 395–535 K. (●) This paper, (○) Varadarajan & Fournelle [21].

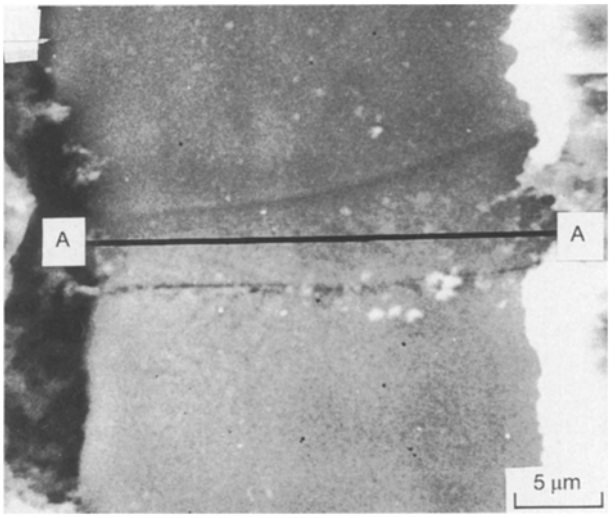

Figure 11 Scanning electron micrograph of Zn–Al–Zn foil couple annealed at 455 K for 10 days. EPMA analysis was performed along line A–A.

3.3. Grain-boundary diffusion

In order to determine the grain-boundary diffusivity, the zinc concentration profiles were measured using EPMA on the samples of B type. Fig. 11 shows an example of such a specimen annealed at 455 K for 10 days. The corresponding zinc distribution along the line A–A is presented in Fig. 12, together with other results obtained in the temperature range from 415–495 K. As can be seen, zinc profiles adopt a U-shape with the maximum zinc content close to the Al–Zn interface and the minimum in the middle of the diffusion couple. The increase of the annealing temperature leads to an increase of C_{max} from 1.3 wt% at 415 K to 3.6 wt % at 495 K and C_{min} from 0.5–2.2 wt %, respectively. The profiles were analysed by solving Cahn's [24] equation, showing the solute distribution $C(Z)$ for the DIGM case

$$C(Z) = C_0 \frac{\cosh(ZA)}{\cosh(SA/2)} \quad (1)$$

where $A = (V/KD_b\lambda)^{0.5}$, Z is the distance measured from the centre of a specimen in a perpendicular direction to its surface, C_0 is the zinc content at the edges of the alloyed zone (i.e. for $Z = \pm S/2$), S is the thickness of the specimen, V is the velocity of GB migration, and $KD_b\lambda$ is the diffusivity at the migrating boundary.

The equation was fitted to the experimental points using a statistical procedure and the final choice is shown by solid curves in Fig. 12. The A values which were thus obtained are given in Table I. Resultant values of diffusivity were calculated using the V values reported in Table I and S values shown in Fig. 12.

4. Discussion

At the beginning, it is necessary to consider whether the investigated process may, or may not be called DIGM. Arguments "against" were introduced by Varadarajan and Fournelle [21]. They did not ob-

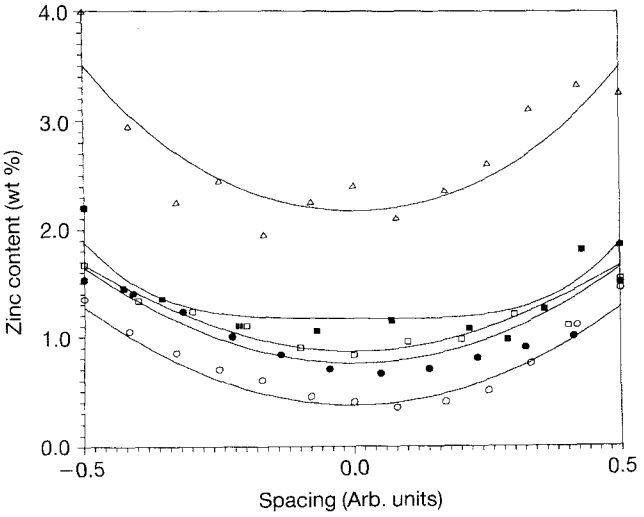

Figure 12 Zinc concentration profiles across Zn–Al–Zn thin foils annealed in the temperature range 415–495 K. (○) 415 K, $S = 24\ \mu m$, $A = 1.9 \times 10^5\ m^{-2}$; (●) 435 K, $S = 16\ \mu m$, $A = 1.8 \times 10^5\ m^{-2}$; (□) 455 K, $S = 16\ \mu m$, $A = 1.41 \times 10^5\ m^{-2}$; (■) 475 K, $S = 14\ \mu m$, $A = 1.5 \times 10^5\ m^{-2}$; (△) 495 K, $S = 12\ \mu m$, $A = 1.73 \times 10^5\ m^{-2}$.

serve any of the microscopic features, such as boundary bowing or S morphology, normally associated with DIGM. Another argument was that the calculated driving force was very small and of the same order of magnitude as the driving force for normal grain growth.

In our study, the S mechanism was observed via SEM. Also, Tashiro and Purdy [19] found similar evidence using TEM. It should be stressed that the DIGM process does not require the presence of the S mechanism. As reviewed by King [25], the boundary topology which develops during DIGM is highly stochastic. In fact, in the present study, some boundaries migrated monotolithically in a single direction while others formed bulges into both grains. Many boundaries remained stationary.

The calculation of the driving force made by Varadarajan and Fournelle [21] was based on the assumption that the only source of the driving force was the coherency strain stored in the zinc concentration profile ahead of the boundary. This results from the estimation of volume penetration distances, D_v/V, ahead of migrating boundaries which were more than one order of magnitude larger than the interatomic distance. Here D_v is the volume diffusion coefficient and V is the velocity of boundary migration. However, the question remains of whether the interface is relaxed enough with respect to volume diffusion so that no chemical driving force acts on the boundaries. Suppose that there is a small compositional gradient (0.5 at %) just at the boundary. Such a gradient could be a source of chemical driving force of 19 J mol^{-1} at 455 °C for an ideal solution model. This value is much larger than the value reported by Varadarajan and Fournelle [21]. Therefore, it is believed that the coherency strain existing in the diffusion zone ahead of the migrating boundary does not have to be the sole driving force. We presume that a mixed driving force may exist with both strain and chemical contribution.

On the other hand, the accuracy of the criterion D_v/V should be discussed. The question is whether it is rigorous and certain or gives us only a superficial view of the tendency of the changes. The DIGM process is a near-surface phenomenon and perhaps the ratio D_v/V fails to give an accurate representation of diffusion in such a case. In our opinion, the arguments yielded by Varadarajan and Fournelle [21] are not sufficient to deny the occurrence of DIGM in the Al–Zn system.

Before discussing the results of chemical analysis and migration rates, some comment concerning the occurrence of the DIGM process is required. It is supposed that a continuous supply of the solute atoms from an outer source is necessary to cause the boundary to move. The number of solute atoms at the migrating boundary depends on two factors: the first is the rate of boundary diffusion which controls a transfer of solute atoms down the boundary; the second factor, migration velocity, controls the flux of atoms normal to the boundary. Mutual contribution of these two factors to the DIGM process results in more solute atoms left behind the boundary or more solute atoms diffusing further along the boundary. The boundary migration rate can also be modified by a significant amount of volume diffusion occurring ahead of the moving front. This leads to a slowing down of the migration process due to a reduced solute flux at the boundary and a small solute concentration gradient across it.

Based on this comment, we will discuss the results obtained in the present paper. The investigation showed the existence of zinc-alloyed zones typical for the DIGM process. Taking into account the maximum migration distance and zinc-enrichment level, DIGM areas were divided into two kinds, laminar and turbulent. Analysis of the chemical composition performed using EPMA showed zinc enrichment at the final position of the migrating boundary. Such behaviour was expected to lead to a reduction of the boundary velocity because the diffusion process was not fast enough to relax the "pinning" forces acting on the migrating boundary. The significant depth to which migration occurs could also be due to this low migration rate. In this case, most of the atoms were not used up by the boundary migration, so that a larger flux may diffuse down the original boundary for a larger distance. The "step-like" changes of zinc-content are within the spatial resolution of the EPMA and it is not possible to draw any quantitative information. A more sophisticated test performed by means of the analytical electron microscope (Fig. 9a,b) offers the spatial resolution two orders of magnitudes better. However, even during this test, the diameter of the X-ray interaction volume calculated using Monte Carlo simulations was found to be about 20 nm. This indicates that the examination could not detect whether or not the volume diffusion occurred within the matrix in the immediate vicinity of the boundary. Therefore, it is supposed that some volume diffusion takes place ahead of the moving boundary but the role of that process is not as important as was expected. The volume diffusion should facilitate a relaxation of the "pinning forces". Calculation of the penetration dis-

tance of volume diffusion, D_v/V, where D_v (Table I) is the volume diffusion coefficient and V is the grain-boundary migration rate, indicated that the effect of volume diffusion should be more pronounced at higher annealing temperatures. D_v values were taken from the data of Hilliard *et al.* [26] for the zinc radio tracer diffusion in diluted Al–Zn solution. An increasing effect of volume diffusion leads to retardation of boundary migration, because the compositional gradient at the boundary is reduced and the chemical contribution to driving force is eliminated. Because V has much lower temperature dependence than D_v, this process is favoured by high temperatures.

During annealing above 450 K the new kind of DIGM, termed turbulent, occurs, which is associated with an excess of solute atoms flux close to the surface of the specimen. This favoured migration of the grain boundary (Fig. 5) could be identified as some kind of diffusion-induced recrystallization (DIR) if it were not for the fact that it was difficult to separate particular grains, in spite of a number of attempts with various etching mixtures. Therefore, it is supposed that a new grain enriched with zinc develops from the original position of the grain boundary (OGB). This new grain nucleates at the junction point and the boundary starts to move. Once motion begins it must be sustained by diffusion of zinc from a reservoir to the grain boundary and then down the boundary. The largest flux is expected to be close to the surface where there is direct contact with the solute source. As a result of this large flux, a relatively sharp change of zinc concentration, ΔC_{Zn}, forms at the interface between the alloyed zone and aluminium which forces the boundary to move. During migration, some of the zinc atoms are deposited behind the boundary and a reduced number can move further along the boundary to the interior of the diffusion couple. The number of solute atoms used to move the boundary decreases with the depth of the material. This was confirmed by results of EPMA analysis, showing that ΔC_{Zn} decreases from 8.0 wt% Zn close to the solute source (Fig. 6a) to 5.5 wt% at a distance of 40 μm (Fig. 6d) and then to 0.4 wt% Zn at a distance of 75 μm (Fig. 6f) from the solute source. This concept is also confirmed by a rough estimation of the migration rate at various depths below the surface. The rate, calculated as a ratio of migration distances to the time of annealing, decreased several times with increasing depth from 5–75 μm.

The decrease of solute content along the migrating boundary diminishes the driving force for the process. At a certain distance below the surface, the driving force disappears and no symptoms of DIGM are observed. It is not clear why the distance of GB migration (Fig. 5) does not decrease monotonically along the depth, showing rather sharp steps at 10 and 25 μm below the surface. A change in GB structure precluding dislocation climb according to the Baluffi–Smith [27, 28] model, is a possible explanation. It is not definitely obvious whether the diffusion of zinc atoms is impossible down the original location of the GB. A network of dislocations left there forms a small-angle boundary which could act as a relatively easy path for diffusion. However, a supplementary experiment is necessary which would allow variation of solute concentration at the original position of the GB for a series of annealing times to be detected.

Relatively sharp change of zinc content at the boundary between matrix and alloyed zone suggests the serious chemical contribution to the total driving force of DIGM. A chemical origin of the driving force is also expected in the case of oscillatory movement. This movement leads to a homogenization of solute distribution in the alloyed zone.

The investigation of sections of Zn–Al–Zn samples (B type) allows large changes of migration distances with depth below the surface to be eliminated, because the solute gradients are levelled out by overlapping the concentration distribution originating from two opposite Zn–Al surfaces of the sample. In such a case, the velocity of GB migration is independent of the distance from the surface. It should be noted that the measured GB velocity in cross-sections of B type samples was comparable to that measured at the surface of oblique sections of an A type sample. Therefore, the values of GB velocity reported in Table I were used to calculate the diffusivity at migrating GBs. The calculated $KD_b\lambda$ products are graphically presented in Fig. 13, together with other data on the diffusion at the migrating boundaries [29–31]. It can be seen that $KD_b\lambda$ values are comparable with the diffusivities at the stationary grain boundary in pure aluminium or diluted (2 at% Zn) AlZn alloy reported by Haessner [32]. The calculated diffusivities are slightly higher than those estimated based on the Tu–Turnbull model [33] for the discontinuous precipitation and dissolution in Al 22 at % Zn alloy [29]. At the same time, the diffusivities of DIGM are approximately ten orders of magnitude higher than the volume diffusion coefficient (see Table I) multiplied by the grain-boundary thickness, λ (assumed to be 5×10^{-10} m) and the

TABLE I

T(K)	V (10^{11} m s^{-1})	D_v (m^2 s^{-1})	D_v/V (m)	A (10^{-5} m^{-2})	$KD_b\lambda$ (m^3 s^{-1})
395	0.10	1.10×10^{-22}	1.10×10^{-10}	–	–
415	1.34	6.16×10^{-22}	4.60×10^{-11}	1.9	3.71×10^{-22}
435	1.82	2.94×10^{-21}	1.62×10^{-10}	1.8	5.61×10^{-22}
455	3.24	1.22×10^{-20}	3.77×10^{-10}	1.41	1.63×10^{-21}
475	4.63	4.50×10^{-20}	9.72×10^{-10}	1.5	2.06×10^{-21}
495	2.80	1.49×10^{-19}	5.32×10^{-9}	1.73	9.36×10^{-22}
515	1.40	4.52×10^{-19}	3.23×10^{-8}	–	–
535	0.20	7.61×10^{-19}	3.81×10^{-7}	–	–

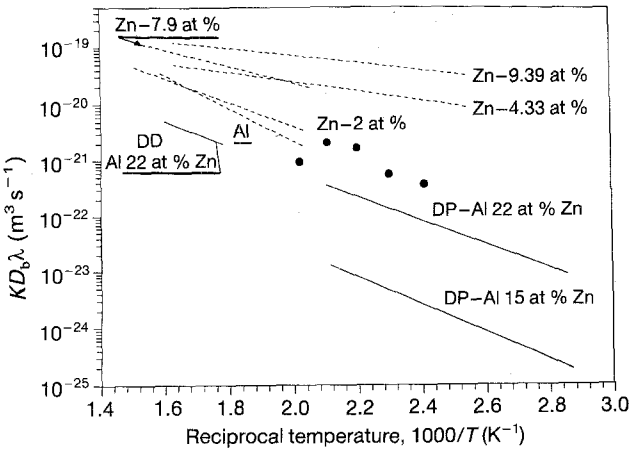

Figure 13 Arrhenius graph for (●) the DIGM process in Zn–Al–Zn diffusion couples annealed in the temperature range 415–495 K. Data on diffusivity at (– – –) a stationary grain boundary [32], discontinuous precipitation in Al 15 at% Zn [30, 31], Al 22 at% Zn alloys [29] and discontinouous dissolution in Al 22 at% Zn alloy [29] are also reported for comparison.

segregation factor, K (taken as $K = 1$). Therefore, it is concluded that the DIGM process is controlled by the diffusion of zinc atoms along the moving grain boundary.

The level of enrichment is much lower in samples of B type. No explanation of this can be offered at the present moment. One can only speculate that there is different proportion between migration and diffusion in very thin samples.

The possible differences between the diffusivities calculated based on the measurements performed for the thin foil and for the bulk specimen can be estimated using a modified Cahn's relation for the bulk specimen

$$C(X) = C_0 \exp[-X(V/KD_b\lambda)^{0.5}] \quad (2)$$

Transforming this equation to

$$\log C(X) = \log C_0 - \frac{1}{(KD_b\lambda)^{1/2}\ln 10} V^{1/2} X \quad (3)$$

it is possible to calculate the diffusivity from a slope of $\log C(X)$ versus X drawn based on Fig. 7. Assuming that the migration rate reported in Table I is valid for the near-surface alloyed layer, the diffusivity was found to be 5.27×10^{-22} $m^3 s^{-1}$ at 455 K. This is almost one order of magnitude smaller than data listed in Table I. Such a result suggests that the method of sample preparation and the thickness of the sample may have serious influence on the kinetics of the DIGM process.

5. Conclusions

Based on the present investigation, it seems that the process observed during annealing of Al–Zn diffusion couples can be identified as DIGM. The following features relevant for this process were found:

1. the formation of two different kinds of zinc-enriched zone, termed laminar and turbulent;

2. an asymmetry of solute profiles with the maximum zinc content at the final position of the boundary;

3. a relatively sharp change of zinc concentration across the boundary ($\Delta C_{Zn} = 3$ wt% at a distance of 50 nm);

4. the diffusivity at the migrating grain boundary during the process is comparable with the diffusivity at the stationary grain boundary in AlZn alloys of zinc content corresponding to the level of zinc enrichment in the DIGM zone. The diffusivity obtained in the present study is slightly higher than during discontinuous precipitation in Al 22 at % Zn alloy.

The laminar kind of DIGM occurs over a wide temperature range (415–515 K) and it is characterized by a small migration distance and a large depth of migration. The zinc enrichment at the sample surface is 4.0–5.0 wt% and gradually decreases with increasing depth. The migration distance exhibits the same tendency.

The turbulent kind of DIGM is limited to annealing temperatures above 450 K. In this case, the width of the alloyed zone is much greater close to the surface of the sample and then dramatically decreases, showing a behaviour similar to the laminar morphology. The zinc content at the surface of the sample is 8.0–9.0 wt%.

The abrupt change of zinc content at the moving boundary and the D_b/D_v ratio around 1×10^{10} indicates that a chemical contribution to the total driving force of DIGM exists.

References

1. M. HILLERT and G. R. PURDY, *Acta Metall.* **26** (1978) 33.
2. LI CHONGMO and M. HILLERT, *ibid.* **29** (1981) 1949.
3. Z. S. YU and P. G. SHEWMON, *Metall. Trans.* **13A** (1981) 1567.
4. P. G. SHEWMON and Z. S. YU, *ibid.* **14A** (1983) 1579.
5. G. MEYRICK, V. S. IYER and P. G. SHEWMON, *Acta Metall.* **33** (1985) 273.
6. V. S. IYER, P. G. SHEWMON and G. MEYRICK, *Scripta Metall.* **20** (1986) 231.
7. LI CHONGMO and M. HILLERT, *Acta Metall.* **30** (1982) 1133.
8. J. W. CAHN, J. D. PAN and R. W. BALUFFI, *Scripta Metall.* **13** (1979) 503.
9. S. MAYER, PhD thesis, University of Stuttgart (1987).
10. T. J. A. DEN DROEDER, *Thin Solid Films* **124** (1985) 135.
11. F. S. CHEN and A. H. KING, *Acta Metall.* **36** (1988) 2827.
12. Z. M. GUAN, G. X. LIU, D. B. WILLIAMS and M. R. NOTIS, *ibid.* **37** (1989) 519.
13. R. SCHMELZE, G. GIAKUPIAN, T. MUSCHIK, W. GUST and R. A. FOURNELLE, *Acta Metall. Mater.* **40** (1992) 997.
14. F. J. A. DEN BROEDER and S. NAKAHARA, *Scripta Metall.* **17** (1983) 399.
15. D. LIU, W. A. MILLER and K. T. AUST, *Acta Metall.* **37** (1989) 3367.
16. C. R. M. GROVENOR, *ibid.* **33** (1985) 579.
17. V. N. LAPOVAK, V. I. NOVIKOV, S. V. SVIRIDA, A. N. SEMENIKHIN and L. I. TRUSOV, *Sov. Phys. Solid State* **25** (1983) 1063.
18. C. R. M. GROVENOR, D. A. SMITH and M. J. GORINGE, *Thin Solid Films* **74** (1980) 269
19. K. TASHIRO and G. R. PURDY, *Scripta Metall.* **21** (1983) 455.

20. G. R. PURDY and K. TASHIRO, in "Interface Migration and Control of Microstructure", edited by D. A. Smith, A. H. King and C. S. Pande (American Soc. Metals, Metals Park, OH, 1986) p. 33.
21. S. VARADARAJAN and R. A. FOURNELLE, *Acta Metall. Mater.* **40** (1992) 1847.
22. R. LÜCK, *Z. Metallkde* **66** (1975) 488.
23. G. CLIFF and G. W. LORIMER, *J. Microscopy* **103** (1975) 203.
24. J. W. CAHN, *Acta Metall.* **7** (1959) 18.
25. A. H. KING, *Int. Mater. Rev.* **32** (1987) 173.
26. J. E. HILLIARD, B. A. AVERBACH and M. COHEN, *Acta Metall.* **7** (1959) 86.
27. R. W. BALUFFI and J. W. CAHN, *ibid.* **29** (1981) 493.
28. D. A. SMITH and A. H. KING, *Philos. Mag.* **A44** (1981) 333.
29. P. ZIEBA and A. PAWŁOWSKI, to be published in *Mat. Sci. Eng.* (1994).
30. A. PAWŁOWSKI, P. ZIĘBA and J. MORGIEL, *Arch. Metall.* **31** (1986) 287.
31. P. ZIĘBA, *Arch. Metall.* **36** (1991) 65.
32. A. HAESSNER, *Kristall Technik* **9** (1974) 1371.
33. K. N. TU and D. B. TURNBULL, *Scripta Metall.* **1** (1967) 173.

Received 13 July 1993
and accepted 21 April 1994